JACS
JOURNAL OF THE AMERICAN CHEMICAL SOCIETY
Article
pubs.acs.org/JACS

Charge-Controlled Switchable CO_2 Capture on Boron Nitride Nanomaterials

Qiao Sun,[†] Zhen Li,*[,‡] Debra J. Searles,*[,†,§] Ying Chen,[∥] Gaoqing (Max) Lu,[⊥] and Aijun Du*[,#]

[†]Centre for Theoretical and Computational Molecular Science, Australian Institute for Bioengineering and Nanotechnology, The University of Queensland, QLD 4072, Brisbane, Australia

[‡]Institute of Superconducting & Electronic Materials, The University of Wollongong, NSW 2500, Australia

[§]School of Chemistry and Molecular Biosciences, The University of Queensland, QLD 4072, Brisbane, Australia

[∥]Institute for Frontier Materials, Deakin University, Waurn Ponds, VIC 3216, Australia

[⊥]ARC Centre of Excellence for Functional Nanomaterials, Australian Institute for Bioengineering and Nanotechnology, The University of Queensland, QLD 4072, Brisbane, Australia

[#]School of Chemistry, Physics and Mechanical Engineering, Queensland University of Technology, Brisbane, QLD 4001, Australia

Supporting Information

ABSTRACT: Increasing concerns about the atmospheric CO_2 concentration and its impact on the environment are motivating researchers to discover new materials and technologies for efficient CO_2 capture and conversion. Here, we report a study of the adsorption of CO_2, CH_4, and H_2 on boron nitride (BN) nanosheets and nanotubes (NTs) with different charge states. The results show that the process of CO_2 capture/release can be simply controlled by switching on/off the charges carried by BN nanomaterials. CO_2 molecules form weak interactions with uncharged BN nanomaterials and are weakly adsorbed. When extra electrons are introduced to these nanomaterials (i.e., when they are negatively charged), CO_2 molecules become tightly bound and strongly adsorbed. Once the electrons are removed, CO_2 molecules spontaneously desorb from BN absorbents. In addition, these negatively charged BN nanosorbents show high selectivity for separating CO_2 from its mixtures with CH_4 and/or H_2. Our study demonstrates that BN nanomaterials are excellent absorbents for controllable, highly selective, and reversible capture and release of CO_2. In addition, the charge density applied in this study is of the order of 10^{13} cm^{-2} of BN nanomaterials and can be easily realized experimentally.

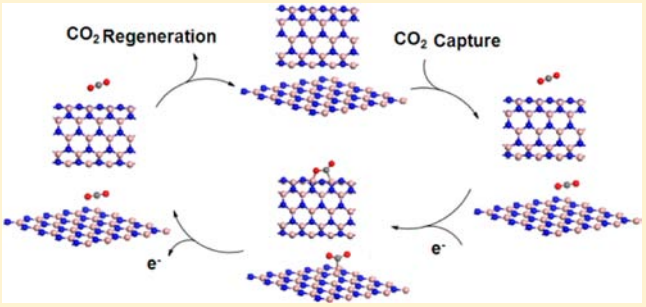

INTRODUCTION

Climate change due to greenhouse emissions has become a significant global challenge, and methods to efficiently and effectively separate, capture, store, and convert greenhouse gases, especially CO_2, have attracted increasing attention.[1−3] CO_2 is a dominant contributor to the greenhouse effect which leads to climate change and global warming.[4,5] The current industrial process for CO_2 capture is based on the use of aqueous amine solutions or chilled ammonia, which suffers from relatively low efficiency and issues such as equipment corrosion, solvent loss, and toxicity.[6] To overcome such disadvantages, solid materials such as metal−organic frameworks (MOFs) and carbon and noncarbon nanotubes have been proposed as attractive adsorbents for CO_2 capture.[6−9] However, a regeneration step in the process of CO_2 adsorption/desorption is required, generally requiring high temperature to release CO_2. In addition, high CO_2 selectivity means that regeneration is difficult due to the large adsorption energy. Therefore, a major challenge for CO_2 capture is to search for a high-performance and low-cost material with high selectivity and easy regeneration.

In recent years, boron nitride (BN) nanomaterials, such as born nitride nanotubes (BNNTs) and nanosheets, have attracted increasing attention due to their unique properties.[10−25] They have excellent mechanical properties, high thermal conductivity, and high resistance to oxidation.[10−15] These properties make them very promising in a variety of potential applications such as optoelectronic nanodevices, spintronics, light emission, photocatalysts, thermal rectifiers, functional composites, etc.[16−21] One potential application is for CO_2 capture and storage.[26] However, the interactions between neutral BN nanosheets, BNNTs, and CO_2 are very weak due to the vacant p-like orbitals of the boron atoms in these materials. In such electron-deficient nanomaterials formation of strong interactions with CO_2 is not favorable because CO_2 is a Lewis

Received: January 9, 2013
Published: May 16, 2013

acid and it prefers to accept, rather than donate, electrons during reaction.

Here, for the first time we demonstrate that by modifying the charge state of the BN nanomaterials adsorption/desorption of CO_2 on BN nanosheets and nanotubes can be controlled and reversed. In contrast to previous reports, the CO_2 capture/release occurs spontaneously without any barriers once the charge is injected into, or dismissed from, BN nanostructures. This is the first report that BN nanomaterials can effectively capture/release CO_2. We also demonstrate the high selectivity of charged BN nanomaterials in separation of CO_2 from gas mixtures such as CO_2/CH_4 and CO_2/H_2. Here we note that the modification of the charge state of BN nanomaterials can be easily realized experimentally using electrochemical methods, electrospray, electron beam, or by gate voltage control.[27−29]

METHODS

The first-principles density-functional theory plus dispersion (DFT-D) calculations were carried out using the DMol3 module in Materials Studio.[30,31] The BN sheet and BNNTs are fully optimized in the given symmetry using the generalized gradient approximation[32] treated by the Perdew−Burke−Ernzerhof exchange-correlation potential with long-range dispersion correction via Grimme's scheme.[33] An all-electron double numerical atomic orbital augmented by d-polarization functions (DNPs) is used as the basis set. The method has been used to successfully determine interactions of some gases and BN nanomaterials.[34] The self-consistent field (SCF) procedure is used with a convergence threshold of 10^{-6} au on the energy and electron density. The direct inversion of the iterative subspace technique developed by Pulay is used with a subspace size 6 to speed up SCF convergence on these systems.[35] Starting with all possible configurations of the gases adsorbed on the BN nanomaterials, geometry optimizations were performed with a convergence threshold of 0.002 au/Å on the gradient, 0.005 Å on displacements, and 10^{-5} au on the energy. The real-space global cutoff radius is set to be 4.10 Å. For the BN sheet, unit cells range from 5 × 5 to 10 × 10, chosen with a 15 Å vacuum between sheets to avoid interactions between periodic images, and the Brillouin zone is sampled by 6 × 6 × 1 k-points using the Monkhorst−Pack scheme. For BNNTs with index from (5, 5) to (10, 10), tetragonal supercells with dimension 30 × 30 × c Å^3 are used, where c is 10.068−10.072 Å and optimized to minimize the energy of the nanotube. The values of lengths of 30 Å were large enough to avoid interactions between periodic images. The Brillouin zones are sampled by 1 × 1 × 6 k-points using the Monkhorst−Pack scheme for six BNNTs.

The adsorption energies of CO_2, CH_4, and H_2 on BN sheets and BNNTs are calculated from eq 1.

$$E_{ads} = (E_{BN} + E_{gas}) - E_{BN\text{-}gas} \quad (1)$$

where $E_{BN\text{-}gas}$ is the total energy of the BN nanomaterials with the adsorbed gas; E_{BN} is the energy of isolated BN sheets and BNNTs; and E_{gas} is the energy of an isolated gas molecule, such as CO_2, CH_4, and H_2. In this paper, the adsorption energy of each configuration is calculated within the same state. The electron distribution and transfer mechanism are determined using the Mulliken method.[36]

The charge densities of CO_2 adsorbed on BN sheets and BNNTs are calculated from eq 2.

$$\rho = \frac{Q}{S} \quad (2)$$

where ρ (10^{13} cm^{-2}) is the electron density of BN sheets and BNNTs; Q is the total charge per unit cell; and S is the surface area of the BN sheets and BNNTs. In addition, the surface area can be calculated from eq 3 and eq 4.

$$S_{(BN\ sheet)} = \frac{\sqrt{3}}{2}a^2 \quad (3)$$

$$S_{(BNNT)} = 2\pi rc \quad (4)$$

where a is the side length of the BN sheets and with values from 12.580 to 25.160 Å for BN sheets with the unit cells from 5 × 5 to 10 × 10; r is the radius of the BNNTs; and c is the length of the BNNTs, which is 10.068−10.072 Å for BNNTs with index from (5, 5) to (10, 10).

RESULTS AND DISCUSSION

First, we performed calculations of CO_2 adsorption on an uncharged BN sheet comprised of a 5 × 5 unit cell with periodic boundaries and a BNNT (5,5). The calculations were carried out using first-principles density-functional theory[32] with long-range dispersion correction (DFT-D).[33] The computational results show that CO_2 molecules can only form weak interactions with these BN nanomaterials. To enhance the ability of CO_2 to be captured on these BN nanomaterials, the charge distributions and electron densities of the BN sheet and BNNT in different charge states were analyzed. Analysis of the results suggests that adding/removing charge to/from the BN nanomaterials allows the control of CO_2 capture and release on/from these BN nanomaterials. To prove the above hypotheses, we studied the adsorption/release of CO_2 on BN sheets and BNNTs carrying different charges. Finally, the separation of CO_2 from gas mixtures of CO_2/CH_4 and CO_2/H_2 using negatively charged BN nanostructures is addressed by comparing the adsorption of CH_4 and H_2 on these nanostructures with that of CO_2.

CO_2 Adsorption on Uncharged BN Sheets and BNNTs. The minimum energy configurations of CO_2 absorbed on the uncharged 5 × 5 BN sheet and BNNT (5,5) are shown in Figure 1. The configuration of the CO_2 and the neutral BN

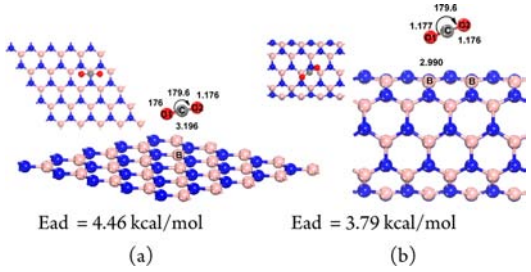

Figure 1. Top and side views of physisorbed CO_2 on a (a) 5 × 5 BN sheet and (b) BNNT (5,5) in their uncharged states. Atom color code: blue, nitrogen; pink, boron; gray, carbon; red, oxygen.

sheet suggests physisorption, and the distance between the carbon atom of CO_2 and boron atom of the BN sheet is 3.196 Å (Figure 1(a)). On physisorption, the linear CO_2 molecule is parallel to the BN sheet, and the absorbed CO_2 molecule shows little structural change compared to a free CO_2 molecule with the O−C−O angle of the absorbed CO_2 being 179.6°. Due to the weak interactions, the charge transfer between the BN sheet and the absorbed CO_2 molecule is negligible with a value of 0.008e^-. These results indicate that the adsorption of CO_2 on the neutral BN sheet is very weak, and the adsorption energy is only 4.46 kcal/mol, which is consistent with the recent report.[26] The weak interaction is mainly attributed to the van der Waals forces between the CO_2 molecule and the BN sorbent. Similarly to the case of the BN sheet, the adsorption of CO_2 on neutral BNNT (5,5) is also a physical process, and the adsorption energy is calculated to be 3.79 kcal/mol. The physical absorption and weak interaction are also attributed to

dx.doi.org/10.1021/ja400243r | J. Am. Chem. Soc. 2013, 135, 8246−8253

the van der Waals interaction between CO_2 and the BNNT. The configuration of the CO_2 adsorbed on BNNT (5,5) is shown in Figure 1(b), and the C···O and B···O bond distances are approximately 3.0−3.4 Å. The linear CO_2 molecule attached to the BNNT is parallel to the B−N bond. The O−C−O angle is very close to 180.0°, which means that the geometry of the physically adsorbed CO_2 is similar to that of free CO_2. The charge transfer between the BNNT and CO_2 is negligible with a value of only 0.002e$^-$. We also investigated CO_2 adsorption on BN sheets comprised of different sized unit cells (from 6 × 6 to 10 × 10) and BNNTs with different diameters (from (6,6) to (10,10)) and found that CO_2 can only form weak interactions with these BN nanomaterials when they are in their neutral states.

Charge Distributions and Electron Densities of Charged BN Sheets and BNNTs. To understand what the influence of changing the charge of the BN nanomaterials might have on the interactions between the BN nanomaterials and CO_2, the electron density distributions of the frontier orbitals (i.e., the lowest unoccupied molecular orbital (LUMO)) for the 5 × 5 BN sheet and BNNT (5,5) are considered in Figure 2(a) and (d), respectively. Figure 2(a) and (d) clearly show that the LUMOs of the BN sheet and BNNT are predominantly distributed on the boron atoms, which suggest that when an extra electron is introduced to the BN nanomaterials the electron will fill the p-like orbitals of boron atoms of the BN sheet and the BNNT, which is confirmed by comparison of the differences in electron density distributions of different charge states of the BN nanomaterials. Figure 2 shows the differences of electron density distributions between the (b) 0e and 1e$^-$ and (c) 0e and 2e$^-$ charged BN sheets, as well as the differences of electron density distributions between (e) 0e and 1e$^-$ and (f) 0e and 2e$^-$ charged BNNTs (5,5). We see from Figure 2 that, when extra electrons are introduced to the BN nanomaterials, the electrons spread across the boron atoms of the BN materials, and then those negatively charged BN adsorbents become more likely to denote electrons to CO_2 (Lewis acid) than their neutral state analogues. The Mulliken charge analysis[36] also supports the above statements. Detailed information on the Mulliken atomic charges of the BN nanomaterial with different charges is listed in Table S1 of the Supporting Information. For the neutral, one electron (1e$^-$) and two electron (2e$^-$) charged 5 × 5 BN sheets, the Mulliken atomic charges of the nitrogen atoms are −0.428e, −0.422e, and −0.415e, respectively. This means that the charge distributions on the nitrogen atoms in the BN sheet are not greatly affected by the change in the total charge of the BN sheet. However, a notable change in boron atomic charge distribution is observed in the negatively charged BN sheet, with the atomic charges of boron atoms in 0e, 1e$^-$, and 2e$^-$ BN sheet being +0.428e, +0.382e, and +0.335e, respectively. The charge populations of boron atoms and nitrogen atoms in BNNT (5,5) with 0e, 1e$^-$, and 2e$^-$ states are similar to those in the case of the BN sheet. In summary, from the above frontier orbital analysis, electron density distributions, and Mulliken atomic charges analysis,[36] it is noted that when extra electrons are added to the BN materials they are distributed on the boron atoms (in preference to the nitrogen atoms). As previously mentioned CO_2 is a Lewis acid and prefers to gain electrons during reaction. The negatively charged BN can donate electrons to CO_2, and their strong interaction is expected. Once the negative charges are released from the BN adsorbents, the negative charge distribution (as shown in Figure 2(b), 2(c), 2(e), and 2(f)) on the boron atoms will vanish simultaneously, and the strong interactions between CO_2 and BN sorbents will disappear. This suggests that switching on/off the charge states of BN nanosheets and nanotubes can control their ability to capture/regenerate CO_2.

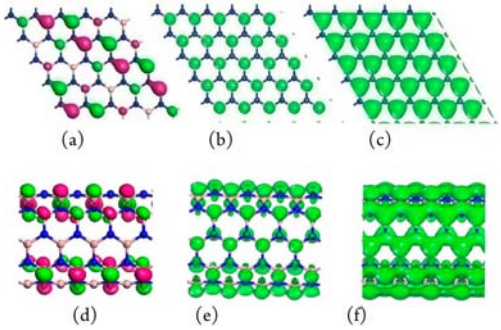

Figure 2. LUMO of (a) 5 × 5 BN sheet and (d) BNNT (5,5). These orbitals are drawn with an isosurface value of 0.03 e/Å^3. The colors of the orbitals show the wave function (green, positive; red, negative). The differences of electron density distributions (b) between 0e and 1e$^-$ as well as (c) between 0e and 2e$^-$ charge carrying states of 5 × 5 BN sheets. The differences of electron density distributions (e) between 0e and 1e$^-$ as well as (f) between 0e and 2e$^-$ charge carrying states of BNNTs (5,5). These densities are drawn with an isosurface value of 0.005 e/Å^3. Atom color code: blue, nitrogen; pink, boron.

CO_2 Adsorption on 1e$^-$ and 2e$^-$ Charged BN Sheets and BNNTs. To prove the above hypotheses, we performed calculations of the adsorption/dissociation of CO_2 on negatively charged BN sheets and BNNTs. After addition of one electron to the 5 × 5 BN sheet, the CO_2 molecule strongly interacts with the BN sheet with an adsorption energy of 18.66 kcal/mol (or 78.37 kJ/mol). Ideally the adsorption energies of CO_2 on high-performance adsorbents should be in a range of 40−80 kJ/mol.[3] According to this criterion, the BN sheet with one negative charge on each 5 × 5 unit cell renders a good sorbent for CO_2 capture. The high adsorption energy indicates strong chemisorption of CO_2 on the negatively charged BN sheet. In the chemisorbed configuration (Figure 3(a)), the CO_2 molecule structure is drastically distorted, and the C atom is bonded with one boron atom in the BN sheet. Compared with the configuration of CO_2 physically adsorbed on the neutral form of the BN sheet (Figure 1(a)), the C−B distance shortened from 3.196 to 2.072 Å; the O−C−O angle bent from around 180° to 139.1°; and the two double C═O bonds are elongated from 1.176 to 1.236 Å. A Mulliken charge population analysis shows that there is 0.570 e$^-$ charge transfer from the BN sheet to the CO_2 molecule.

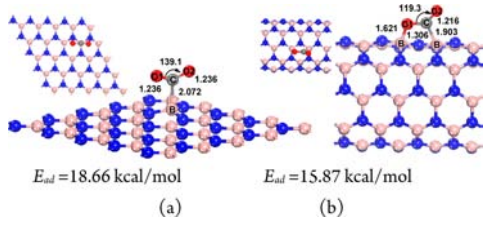

Figure 3. Top and side views of chemisorbed CO_2 on 1e$^-$ charge carrying state of a (a) 5 × 5 BN sheet and (b) BNNT (5,5). Atom color code: blue, nitrogen; pink, boron; gray, carbon; red oxygen.

dx.doi.org/10.1021/ja400243r | J. Am. Chem. Soc. 2013, 135, 8246−8253

The variation of thermodynamic properties, such as change in Gibbs free energy (ΔG, kcal/mol), enthalpy (ΔH, kcal/mol), and entropy (ΔS, cal/(mol K)), with temperature (K) has been calculated (Figure 4) to study the entropic and temperature

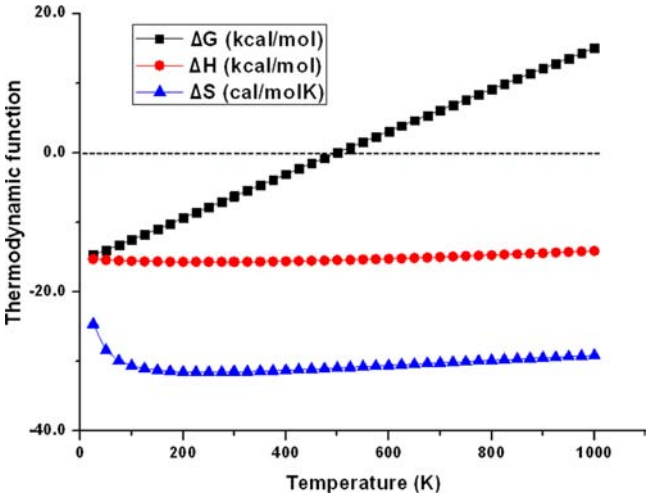

Figure 4. Variation of thermodynamic properties with temperatures (K) when an isolated CO_2 molecule is chemisorbed by a $1e^-$ charged BN sheet. Squares, triangles, and circles correspond to the change in Gibbs free energy (kcal/mol), change in entropy (cal/(mol K)), and change in enthalpy (kcal/mol), respectively.

effects on CO_2 adsorption on the BN sheet ($1e^-$). Figure 4 shows that ΔS decreases with temperature increasing from 25 to 200 K, and ΔS is almost constant when the temperature is above 200 K. The value of ΔH is almost constant over the whole temperature range (i.e., from 25 to 1000 K). This results in ΔG linearly increasing with an increase in temperature. Moreover, ΔG is negative in the temperature range of approximately 25 to 500 K, which indicates the adsorption of CO_2 on the $1e^-$ charged BN sheet to form a chemisorbed configuration is a spontaneous process when the temperature is below 500 K.

Similarly, the CO_2 molecule can also be chemically adsorbed on the surface of negatively charged BNNTs (Figure 3(b)). The adsorption energy is calculated to be 15.87 kcal/mol (66.97 kJ/mol) based on the DFT-D level of calculations. The high adsorption energy also indicates the excellent potential of BNNTs for adsorbing CO_2. A Mulliken charge population analysis shows there is 0.449 e^- charge transfer from BNNT to the CO_2 molecule, which also supports the strong interactions between them. In this case (Figure 3(b)), the CO_2 molecule is distorted, and one double bond is broken. The O−C−O bond angle is 119.3°, and the broken C−O bond is significantly elongated to 1.306 Å on the top of the nanotube. The B sites are also considerably pulled out of the tube, and B−N bonds are increased by 0.20 Å. The B−C and B−O distances are 1.903 and 1.621 Å, respectively.

The higher adsorption energy and distortion of configurations reflect the stronger interactions between CO_2 and the negatively charged BN sheet/NT than with the neutral forms. The enhanced interactions can be explained from the frontier orbitals analysis, electron density distributions, and Mulliken charge populations of the BN sheet/NT. It can be seen that, with extra electrons, boron atoms in the BN nanomaterials become less positively charged than in the neutral nanomaterials. These boron atoms are therefore likely to donate electrons to the CO_2 (Lewis acid), enabling the formation of stronger bonds.

In Figure 5(a) and (c) we start with the minimum energy configuration of the neutral BN sheet and BNNT with

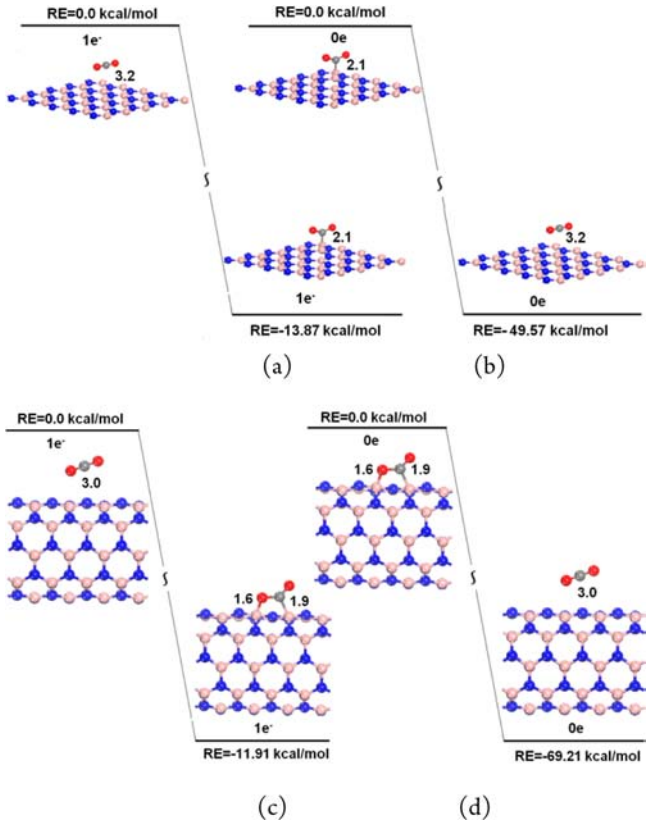

Figure 5. In (a) and (b) energy changes for reactions involving CO_2 adsorption on a 5 × 5 BN sheet are shown. In (a) the change is from physisorption to chemisorption with the BN sheet in a $1e^-$ charge state, and in (b) the change is from chemisorption to physisorption with the BN sheet in a 0e charge state. In (c) and (d) energy changes are shown for CO_2 adsorption on BNNT (5,5) in a (c) $1e^-$ charge state and (d) neutral charge state. Atom color code: blue, nitrogen; pink, boron; gray, carbon; red, oxygen.

physisorbed CO_2. An electron is then added to the BN sheet or NT, and we consider the change in energy as it relaxes to the chemisorbed state. In Figure 5(b) and (d) we start with the minimum energy configuration of the negatively charged BN sheet and BNNT with chemisorbed CO_2. An electron is removed, and then the system is allowed to relax, forming physisorbed CO_2. When an extra electron is introduced to the BN sheet and BNNT, the interactions between CO_2 and BN nanomaterials drastically increase compared with those with the neutral BN sheet and BNNT, and CO_2 molecules are chemisorbed on the BN adsorbents (Figure 5(a) and (c)). The processes are exothermic by 13.87 and 11.91 kcal/mol for the BN sheet and BNNT, respectively, with no barrier. On the other hand, after a negative charge is removed from the systems the adsorption of CO_2 on BN adsorbents spontaneously changes from chemisorption into physisorption without any reaction barrier, and those processes are exothermic with values of 49.57 and 69.21 kcal/mol for the BN sheet and BNNT, respectively. Again the reactions have no barriers to these changes after the electron is removed (Figure 5(b) and (d)). Here it should be noted that the energy for triggering the

dx.doi.org/10.1021/ja400243r | J. Am. Chem. Soc. 2013, 135, 8246−8253

adsorption/desorption totally relies on the energy used for charging/discharging of the BN absorbents. Once the charge states were switched on/off, both adsorption and desorption processes of CO_2 on BN adsorbents seem to be spontaneous. In summary, our calculations indicate the BN sheet and BNNT could be new adsorbent materials for controlled capture and release of CO_2 because they can be easily charged and discharged by electrochemical methods, electrospray, electron beam, or gate voltage control.

To know whether CO_2 can absorb on negatively charged BN sheets with larger unit cells and BNNTs with bigger diameters, we investigate the CO_2 adsorption on different sized BN sheets and BNNTs. Calculations were carried out on BN sheets with unit cells from 6 × 6 to 10 × 10 and BNNTs with indices from (6,6) to (10,10). The BN sheet lattices are 12.6∼25.2 Å, and BNNT diameters are 6.8∼14.0 Å. Tables S2 and S3 (Supporting Information) list the important structural and energetic properties of CO_2 adsorption on the BN absorbents with different sizes and structures, including bond distances, bond angles, and electron transfer (e^-) from the BN sheet/NTs to CO_2 as well as their adsorption energies. Figure 6 shows the

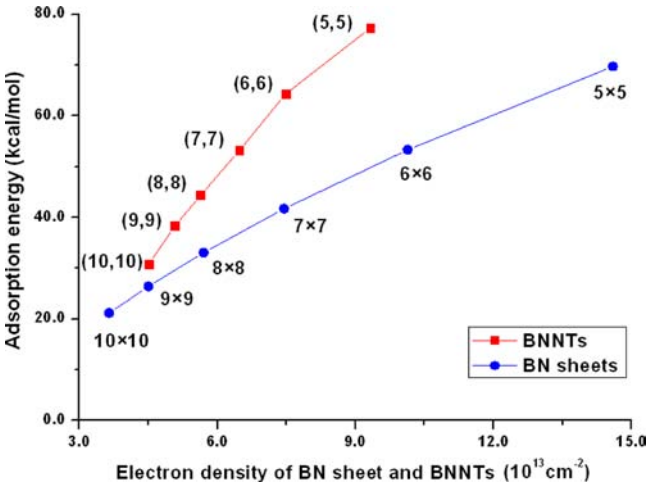

Figure 6. Adsorption energies (kcal/mol) of CO_2 on BN sheets with different unit cell sizes and different BNNTs diameters are shown as functions of electron densities (10^{13} cm^{-2}). The charge state ($2e^-$) is the same for all the computational results shown in the figure.

adsorption energies of CO_2 on different sized BN sheets and different diameter BNNTs as functions of their charge densities. For neutral BN sheets/NTs, CO_2 molecules weakly interact with them by physisorption, and the adsorption energies are around 4 kcal/mol for all BN adsorbents. The charge transfer between CO_2 and BN sheets/NTs is negligible with the values around 0.005e^-. However, for one-electron charged BN sheets with unit cells from 5 × 5 to 8 × 8 and BNNTs with index from (5,5) to (7,7), CO_2 molecules and BN adsorbents chemisorb, and the adsorption energies are 18.66, 13.94, 10.35, and 7.46 kcal/mol for BN sheets with unit cells 5 × 5, 6 × 6, 7 × 7, and 8 × 8 and 15.87, 10.74, and 6.42 kcal/mol for BNNTs with index (5,5), (6,6), and (7,7), respectively. We can see that with an increase of the BN sheet unit cell from 5 × 5 to 8 × 8 and BN diameters from (5,5) to (7,7) the adsorption energies, the charge transfer, and the interactions between CO_2 and BN sheets/BNT decrease gradually. When the unit cell of the BN sheet is 9 × 9 or 10 × 10, the interactions between CO_2 and the BN sheet are very weak. Similarly, when the diameter of the BNNTs is larger than 11.0 Å (with nanotube index (8,8)), CO_2 molecules are physically adsorbed on the singly charged BNNTs with an adsorption energy of 3.90 kcal/mol, which is very similar to the adsorption of CO_2 on the neutral state BNNT (8,8). This can be understood from the viewpoint of charge states. When the size of the BN sheets and BNNTs increases, the positive charge of the boron atoms is increased, resulting in weaker interactions between boron atoms of BN sheets/NTs and CO_2. The electrons allocated to the boron atoms can significantly influence the adsorption characteristics of CO_2 on BN sheets/NTs, as demonstrated computationally by considering the results from different sized BN sheets/NTs charged with two electrons. Stronger interactions formed between CO_2 and all BN sheets/NTs when charged with $2e^-$ (Tables S2 and S3 in the Supporting Information list the detailed information of the charge state). The adsorption energies between them are 69.73−21.13 kcal/mol with the lattice of the BN sheet increasing from 12.6 to 25.2 Å. Absorption energies of 77.27−30.84 kcal/mol are obtained when the diameter of the BNNTs increases from 6.8 to 14.0 Å, respectively. It means that if two negative charges are located on each unit cell BN nanomaterials with relative larger size can also efficiently capture CO_2.

In those calculations, there is one CO_2 molecule on each BN adsorbent, so the calculations with higher coverages of CO_2 have been carried out. Table S4 and Figure S1 in the Supporting Information list the structural properties and average adsorption energies (kcal/mol) with different coverages of CO_2 on BN sheets with a 6 × 6 unit cell and a $2e^-$ charge state and up to nine molecules of CO_2 (a coverage of 0.25 molecules per B atom). We find that the average adsorption energies of CO_2 on the BN sheet decrease from 53.31 to 4.72 kcal/mol with an increase in CO_2 coverage from 0.03 to 0.25 CO_2 molecules per boron atom. The configurations of the CO_2 adsorbed on the BN sheet are also consistent with a change from chemisorption to physisorption with the increase in CO_2 coverage.

The adsorption energies of CO_2 on BN sheets with different sized unit cells and BNNTs with different diameters, as a function of the electron densities, are shown in Figure 6. We can see that the adsorption energies of CO_2 on BN adsorbents depend almost linearly on their electron densities. The adsorption energy of the BNNTs increases more rapidly than that of the BN sheets because of the curvature of BNNTs, which increases as the diameter becomes smaller. These results further demonstrate the feasibility of capturing/releasing CO_2 by using charged/uncharged BN nanostructures, even for large BN sheets/NTs. As mentioned previously, the charge densities used in this study, which are of the order of 10^{13} cm^{-2} of BN nanomaterial, can be easily achieved, e.g., by using electrochemical method, electrospray, electron beam, or gate voltage control.[27−29] For example, a charge density of 7.4 × 10^{13} cm^{-2} has been obtained with the most common gate.[29]

CH_4 and H_2 Adsorption on BN Sheets and BNNTs. To demonstrate the high selectivity of negatively charged BN nanostructures for CO_2 adsorption, the adsorption energies of CH_4 and H_2 on charged and discharged 5 × 5 BN sheets and BNNTs (5,5) are calculated and compared with that of CO_2. The results indicate that the adsorption of CH_4 and H_2 on these BN nanomaterials under all conditions considered is physical rather than chemical. Table S5 (Supporting Information) displays the important parameters for these

dx.doi.org/10.1021/ja400243r | J. Am. Chem. Soc. 2013, 135, 8246−8253

physical adsorptions, such as bond distances, adsorption energies, and electron transfer from BN nanomaterials to CH_4 and H_2. The C···B distances for CH_4 adsorbed on BN nanostructures are between 3.4 and 3.6 Å, and H···B distances for H_2 absorption are in a range of 2.4−2.7 Å. Figure 7

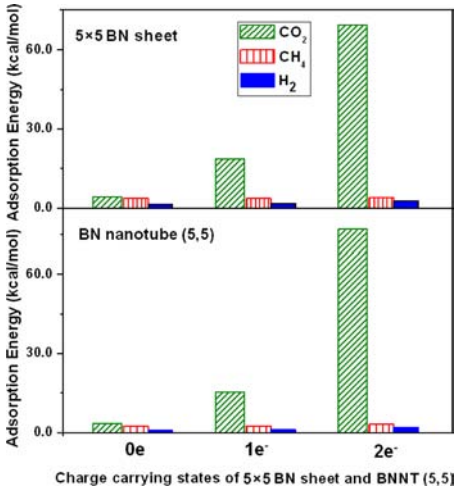

Figure 7. Adsorption energies (kcal/mol) of CO_2, CH_4, and H_2 adsorbed on 5 × 5 BN sheets and BNNTs (5,5) with neutral, $1e^-$, and $2e^-$ charge states.

compares the adsorption energies of CO_2, CH_4,and H_2 on BNNT (5,5) and a BN sheet with neutral, $1e^-$, and $2e^-$ charged states. For the neutral 5 × 5 BN sheet and BNNT (5,5), CH_4 and H_2 physically adsorb, and the adsorption energies are around 2−3 kcal/mol for CH_4 and 1−2 kcal/mol for H_2, respectively. The interactions are similar to those of the CO_2 molecules with neutral BN sheets and BNNTs. When BN nanostructures are injected with one electron and two electrons, the adsorption of CH_4 and H_2 on them remains physical, and the change of adsorption energies is very small in comparison to neutral BN materials. In contrast, the absorption of CO_2 on one-electron charged BN sheets and BNNTs is much stronger. Their chemisorption energies are 18.66 and 15.87 kcal/mol for the BN sheet and BNNT (5,5), respectively. With two extra electrons, the interactions between CO_2 and the BN sheet and BNNT become very strong, and the adsorption energies are increased to 69.73 and 77.27 kcal/mol for the BN sheet and BNNT (5,5), respectively. The charge transfer from the $2e^-$ charged BN sheet and BNNT to the CO_2 molecules also increases significantly, with charge transfer values of $0.717e^-$ and $0.983e^-$, respectively. For BN nanostructures charged with two electrons, a CO_2 molecule binds more tightly with them than those charged with one electron. In the chemisorption process, CO_2 molecules undergo significant structural distortion (Table S2 and S3Supporting Information), in which the C−B bond between the C atom in CO_2 and the B atom in the BN sheet and BNNT becomes shorter with a length of 1.670 and 1.666 Å, respectively. The O−C−O angles of CO_2 molecules adsorbed on the BN sheet and BNNT are bent to 119.5° and 124.9°, respectively. The above comparisons demonstrate that negatively charged BN sheets and BNNTs have very high selectivity for capturing CO_2 from CH_4 and H_2 mixtures, and these nanostructures can serve as good adsorbents for separation of these gases.

CO_2 and Gas Mixture Adsorption on a BN Sheet with an Electric Field. To further demonstrate the reaction mechanism of charge-controlled adsorption/dissociation of CO_2 on BN nanomaterials, the calculations of CO_2 capture and release and gas mixture (CO_2, CH_4, and H_2) separation controlled by switching on and off an electric field (0.05 au)[37] of the systems have been carried out. First we discuss CO_2 capture/release on the BN sheet by switching on and off the electric field. The optimized geometrical parameters and adsorption energies of the physisorption (a) and chemisorption (b) configurations for CO_2 adsorption on the 5 × 5 BN sheet without and with the electric field are presented in Figure S2 in the Supporting Information. In its physisorption (Figure S2(a)) and chemisorption (Figure S2(b)) configurations, the distances between the boron atom in the BN sheet and one oxygen atom in the CO_2 molecule are 3.001 and 1.651 Å, and the their adsorption energies are calculated to be 2.41 and 19.26 kcal/mol, respectively, which suggests CO_2 strongly interacts with the BN sheet in the presence of the electric field. Figure 8(a) shows the temperature dependence of thermodynamic properties, such as ΔG (kcal/mol), ΔH (kcal/mol), and ΔS (cal/(mol K)), of the adsorption reaction of CO_2 on the BN sheet with

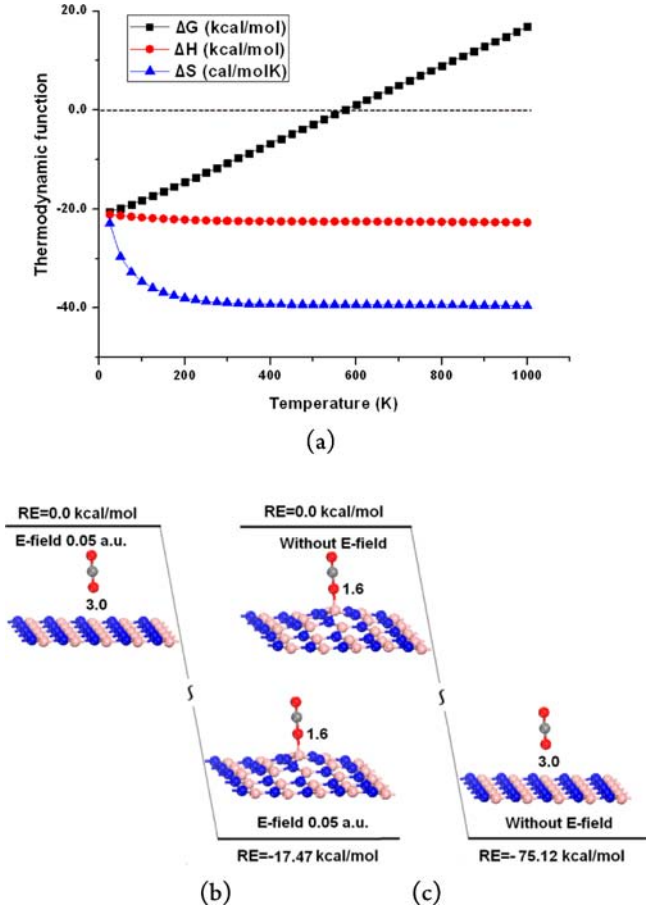

Figure 8. (a) Variation of thermodynamic properties with temperatures (K) when an isolated CO_2 molecule adsorbs on a BN sheet to form chemisorption configuration with a vertical electric field of 0.05 au. Squares, triangles, and circles correspond to the change in Gibbs free energy (kcal/mol), change in entropy (cal/(mol K)), and change in enthalpy (kcal/mol), respectively. (b) The energy change due to a change from the physisorbed to chemisorbed configurations with an electric field of 0.05 au on a 5 × 5 BN sheet. (c) The energy change due to a change from chemisorbed to physisorbed configurations without an electric field for CO_2 adsorption on the 5 × 5 BN sheet.

dx.doi.org/10.1021/ja400243r | J. Am. Chem. Soc. 2013, 135, 8246−8253

the electric field. It clearly shows that the ΔS of the reaction decreases first and then reaches a constant with temperature increasing from 200 to 1000 K. Thus ΔG of this reaction increases with the increase of temperature. Moreover, the negative ΔG below 600 K indicates the adsorption reaction process is spontaneous when the temperature is below 600 K.

Figure 8(b) and (c) schematically shows two reaction processes. In (b), we start with the minimum energy physisorption configuration that the system would adopt without an electric field (Figure S2(a), Supporting Information). Next an electric field is applied, and then the system is allowed to relax. In (c) we start with the minimum energy chemisorption configuration that the system would adopt when the electric field is on (Figure S2(b), Supporting Information). The electric field is then switched off, and the system is allowed to relax. When the electric field is applied to the system, the interactions between CO_2 and the BN sheet drastically increase compared with the case without the electric field, and the CO_2 molecule is chemisorbed on the BN sheet (Figure 8(b)). The process is exothermic by 17.47 kcal/mol without a reaction barrier. On the other hand, when the electric field is switched off, adsorption of CO_2 on the BN sheet changes from chemisorption into physisorption without any reaction barrier, and the process is exothermic by 75.12 kcal/mol (Figure 8(c)). Similar to the reaction mechanism of charged-controlled CO_2 capture/release on the BN materials, the processes of CO_2 capture/release in the presence/absence of an electric field (0.05 au) are found to be also spontaneous. There is an energy cost to the process since it strongly depends on switching on/off an electric field. The CO_2 capture/release controlled by charging/discharging should be very similar to that controlled by switching on/off an electric field, and the energy cost mainly comes from adding/removing the charges to/from the adsorbents experimentally.

In addition, the adsorption of a gas mixture (one molecule of CO_2, H_2, and CH_4) on the BN sheet in the presence/absence of the electric field has also been calculated to address the gas separation by applying an electric field on the material. The physisorption and chemisorption configurations of the gas mixture on the BN sheet without and with the electric field, the thermodynamic properties of the reaction from isolated gases to chemisorption, and the reaction energies for switching on and off the electric field for physisorption and chemisorption configurations are demonstrated in Figures S3–S5 in the Supporting Information, respectively. The adsorption energies of the gas mixture on the BN sheet for the two configurations (Figure S3(a)) without and (Figure S3(b)) with electric field are 8.20 and 29.89 kcal/mol, respectively. From the two optimized configurations (Figure S3(a) and Figure S3(b)) of gas mixture adsorption on the BN sheet, we can see that the CO_2 molecule changes from far binding to the BN sheet to tight binding with the B–O bond distances shortening from 2.995 to 1.651 Å. However, the distances of H_2 and CH_4 to the BN sheet are almost unaffected by switching on and off the electric field, which demonstrates that CO_2 can be efficiently separated from the gas mixture by applying the electric field. The energy profiles of reaction processes (Figure S5 in the Supporting Information) of applying electric field to the physisorption configuration (Figure S5(a)) and switching off the electric field with the chemisorption configuration (Figure S5(b)) indicate these processes have no energy barrier. Moreover, ΔG for adsorption of the gas mixture on the BN sheet by applying an electric field is negative around 300 K (Figure S4 in the Supporting Information), which indicates that the chemisorption of CO_2 in the presence of H_2 and CH_4 with the electric field is spontaneous at room temperature.

CONCLUSIONS

In summary, the adsorption/desorption of CO_2 on charged and discharged BN sheets and BNNTs was theoretically investigated. The results show that CO_2 adsorption on BN nanostructures can be drastically enhanced by introducing electrons to the adsorbent. The absorbed CO_2 can be spontaneously released from BN nanosorbents without any reaction barrier once the electrons are removed. The results suggest that negatively charged BN nanomaterials are excellent sorbents for CO_2, and they can be used to separate CO_2 from gas mixtures, in processes such as natural gas sweetening (CO_2/CH_4) and postgasification (CO_2/H_2) capture. These results are also supported by the calculations on the adsorption/desorption of CO_2 and gas mixture separation on the BN nanostructure in the presence/absence of an electric field. Our investigation demonstrates a versatile approach to CO_2 capture, regeneration, and gas separation by charging/discharging the sorbents which can be easily realized.

ASSOCIATED CONTENT

Supporting Information

Mulliken atomic charges of the BN nanomaterial with different charges and important structural properties as well as adsorption energies of the gas adsorption on the different size and different charge states of BN nanomaterials. This material is available free of charge via the Internet at http://pubs.acs.org.

AUTHOR INFORMATION

Corresponding Author

zhenl@uow.edu.au (Z.L.); d.bernhardt@uq.edu.au; (D.J.S.); aijun.du@qut.edu.au (A.D.)

Author Contributions

All authors have given approval to the final version of the manuscript.

Notes

The authors declare no competing financial interest.

ACKNOWLEDGMENTS

We are grateful to the Australian Research Council for supporting this work. Q.S. acknowledges financial support from Early Career Researcher grant of The University of Queensland. A.D. greatly appreciates financial support of the Australian Research Council QEII Fellowship. We also acknowledge generous grants of high performance computer time from both The University of Queensland and the National Computational Infrastructure (NCI).

REFERENCES

(1) Haszeldine, R. S. *Science* **2009**, *325*, 1647.
(2) Keith, D. W. *Science* **2009**, *325*, 1654.
(3) Chu, S.; Majumdar, A. *Nature* **2012**, *488*, 294.
(4) Meyer, J. *Nature* **2008**, *455*, 733.
(5) Betts, R. A.; Boucher, O.; Collins, M.; Cox, P. M.; Falloon, P. D.; Gedney, N.; Hemming, D. L.; Huntingford, C.; Jones, C. D.; Sexton, D. M. H.; Webb, M. J. *Nature* **2007**, *448*, 1037.
(6) Ferey, G.; Serre, C.; Devic, T.; Maurin, G.; Jobic, H.; Llewellyn, P. L.; De Weireld, G.; Vimont, A.; Daturi, M.; Chang, J.-S. *Chem. Soc. Rev.* **2011**, *40*, 550.

(7) Furukawa, H.; Ko, N.; Go, Y. B.; Aratani, N.; Choi, S. B.; Choi, E.; Yazaydin, A. O.; Snurr, R. Q.; O'Keeffe, M.; Kim, J.; Yaghi, O. M. *Science* **2010**, *329*, 424.
(8) Cinke, M.; Li, J.; Bauschlicher, C. W.; Ricca, A.; Meyyappan, M. *Chem. Phys. Lett.* **2003**, *376*, 761.
(9) Wang, B.; Cote, A. P.; Furukawa, H.; O'Keeffe, M.; Yaghi, O. M. *Nature* **2008**, *453*, 207.
(10) Paine, R. T.; Narula, C. K. *Chem. Rev.* **1990**, *90*, 73.
(11) Loiseau, A.; Willaime, F.; Demoncy, N.; Hug, G.; Pascard, H. *Phys. Rev. Lett.* **1996**, *76*, 4737.
(12) Chopra, N. G.; Luyken, R. J.; Cherrey, K.; Crespi, V. H.; Cohen, M. L.; Louie, S. G.; Zettl, A. *Science* **1995**, *269*, 966.
(13) Golberg, D.; Bando, Y.; Tang, C.; Zhi, C. *Adv. Mater.* **2007**, *19*, 2413.
(14) Golberg, D.; Bando, Y.; Huang, Y.; Terao, T.; Mitome, M.; Tang, C.; Zhi, C. *ACS Nano* **2010**, *4*, 2979.
(15) Corso, M.; Auwarter, W.; Muntwiler, M.; Tamai, A.; Greber, T.; Osterwalder, J. *Science* **2004**, *303*, 217.
(16) Chen, Y.; Zou, J.; Campbell, S. J.; Le Caer, G. *Appl. Phys. Lett.* **2004**, *84*, 2430.
(17) Du, A.; Chen, Y.; Zhu, Z.; Amal, R.; Lu, G. Q.; Smith, S. C. *J. Am. Chem. Soc.* **2009**, *131*, 17354.
(18) Du, A.; Chen, Y.; Zhu, Z.; Lu, G.; Smitht, S. C. *J. Am. Chem. Soc.* **2009**, *131*, 1682.
(19) Chang, C. W.; Okawa, D.; Majumdar, A.; Zettl, A. *Science* **2006**, *314*, 1121.
(20) Kubota, Y.; Watanabe, K.; Tsuda, O.; Taniguchi, T. *Science* **2007**, *317*, 932.
(21) Levendorf, M. P.; Kim, C.-J.; Brown, L.; Huang, P. Y.; Havener, R. W.; Muller, D. A.; Park, J. *Nature* **2012**, *488*, 627.
(22) Chen, W.; Li, Y.; Yu, G.; Li, C.-Z.; Zhang, S. B.; Zhou, Z.; Chen, Z. *J. Am. Chem. Soc.* **2010**, *132*, 1699.
(23) Hao, S.; Zhou, G.; Duan, W.; Wu, J.; Gu, B.-L. *J. Am. Chem. Soc.* **2008**, *130*, 5257.
(24) Li, J.; Zhou, G.; Chen, Y.; Gu, B.-L.; Duan, W. *J. Am. Chem. Soc.* **2009**, *131*, 1796.
(25) Hu, S. L.; Zhao, J.; Jin, Y. D.; Yang, J. L.; Petek, H.; Hou, J. G. *Nano Lett.* **2010**, *10*, 4830.
(26) Choi, H.; Park, Y. C.; Kim, Y.-H.; Lee, Y. S. *J. Am. Chem. Soc.* **2011**, *133*, 2084.
(27) Kanai, Y.; Khalap, V. R.; Collins, P. G.; Grossman, J. C. *Phys. Rev. Lett.* **2010**, 104.
(28) Ramesh, P.; Itkis, M. E.; Bekyarova, E.; Wang, F.; Niyogi, S.; Chi, X.; Berger, C.; de Heer, W.; Haddon, R. C. *J. Am. Chem. Soc.* **2010**, *132*, 14429.
(29) Novoselov, K. S.; Geim, A. K.; Morozov, S. V.; Jiang, D.; Katsnelson, M. I.; Grigorieva, I. V.; Dubonos, S. V.; Firsov, A. A. *Nature* **2005**, *438*, 197.
(30) Delley, B. *J. Chem. Phys.* **1990**, *92*, 508.
(31) Delley, B. *J. Chem. Phys.* **2000**, *113*, 7756.
(32) Perdew, J. P.; Burke, K.; Ernzerhof, M. *Phys. Rev. Lett.* **1996**, *77*, 3865.
(33) Grimme, S. *J. Comput. Chem.* **2006**, *27*, 1787.
(34) Wu, X.; An, W.; Zeng, X. C. *J. Am. Chem. Soc.* **2006**, *128*, 12001.
(35) Pulay, P. *J. Comput. Chem.* **1982**, *3*, 556.
(36) Mulliken, R. S. *J. Chem. Phys.* **1955**, *23*, 1833.
(37) Zhou, J.; Wang, Q.; Sun, Q.; Jena, P.; Chen, X. S. *Proc. Natl. Acad. Sci. USA* **2010**, *107*, 2801.